Cellulose (2024) 31:321–333
https://doi.org/10.1007/s10570-023-05664-0

ORIGINAL RESEARCH

Green oleogels based on elm pulp cellulose nanofibers: effect of the nanofibrillation pre-treatment on their thermo-rheological behavior

Claudia Roman · Miguel A. Delgado · Samuel D. Fernández-Silva · Moisés García-Morales

Received: 15 May 2023 / Accepted: 29 November 2023 / Published online: 12 December 2023

Abstract Sustainable lubricating oleogels were obtained based on elm (*Ulmus minor* Mill.) pulp cellulose nanofibers in castor oil. Before their nanofibrillation, two samples of the same bleached pulp were subjected to two different pre-treatments, either mechanical PFI (Paper and Fibre Research Institute) refining or chemical TEMPO-mediated oxidation. Their effect on the oleogels' viscous flow and oscillatory shear behaviors was determined at different temperatures. Very pronounced differences were observed between these oleogels. The oleogel from the chemically-pretreated nanofibers showed evidences of being much more sensitive to both temperature and large shear deformations. Hence, its shear modulus underwent a very remarkable decay of 95.8% when subjected to a non-linear stress value of 100 Pa for 30 min. In turn, under the same conditions, a decay of only 41.4% was observed for the oleogel based on the nanofiber from the mechanically-pretreated nanofibers.

C. Roman · M. A. Delgado · S. D. Fernández-Silva · M. García-Morales (✉)
Departamento de Ingeniería Química, Centro de Investigación en Tecnología de Productos y Procesos Químicos (Pro2TecS), Campus de "El Carmen", Universidad de Huelva, 21071 Huelva, Spain
e-mail: moises.garcia@diq.uhu.es

C. Roman
e-mail: claudia.roman@diq.uhu.es

M. A. Delgado
e-mail: miguel.delgado@diq.uhu.es

S. D. Fernández-Silva
e-mail: samuel.fernandez@diq.uhu.es

Graphical abstract

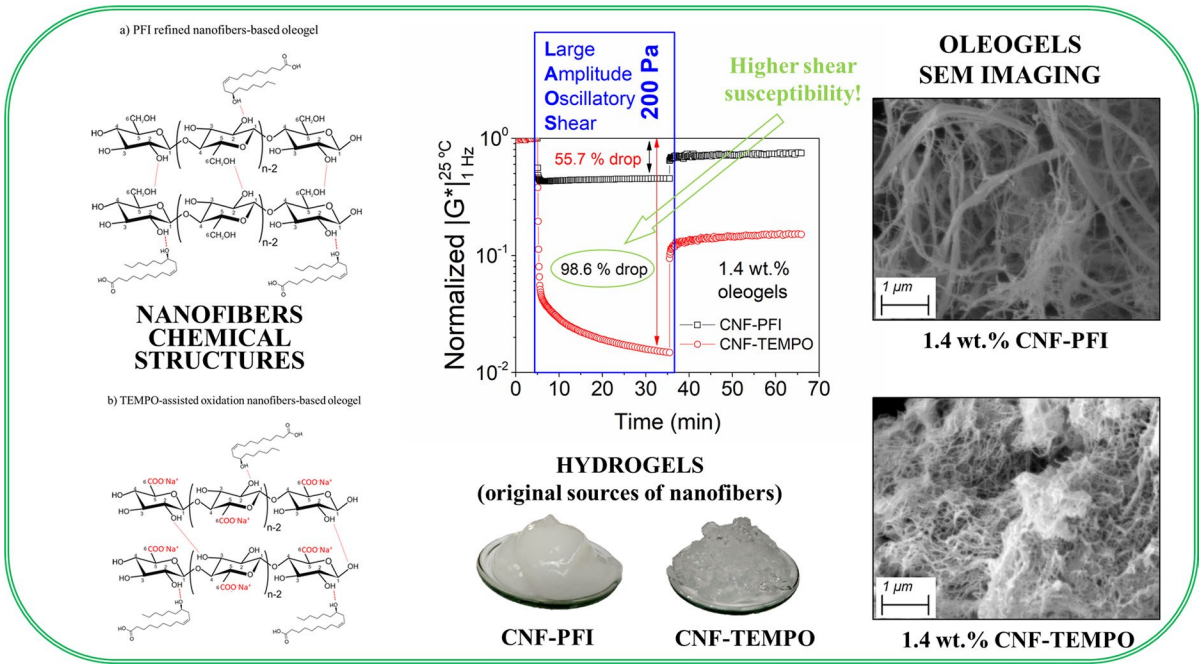

Keywords Cellulose · Nanofiber · castor oil · Sustainability · Rheology · Lubricant

Introduction

The growing demand for eco-friendly products, in general, has reached the lubricants industry as well (Cecilia et al. 2020). Lubricating greases are extensively used in many industrial sectors where reduced friction and wear are needed. An appropriate lubricating grease enables machinery to work without premature failure, and increases machine uptime, productivity and efficiency, thus saving energy and reducing pollutants emission (Bart et al. 2013; Delgado et al. 2020a). Most lubricating greases are constituted by mineral oil and thickeners, in a proportion up to 30 wt% (Domínguez et al. 2021; Reeves et al. 2017). Most of these components are non-biodegradable. The lubrication role is mainly performed by the lubricating oil (Roman et al. 2016). Furthermore, the chemical composition and content of the thickener, which prevents the loss of lubricant under operating conditions, is responsible for the grease's consistency and mechanical stability (Delgado et al. 2019).

The increase in demand for biodegradable lubricants is related to more restrictive rules being implemented to minimize environmental impact caused by inappropriate disposal (Cecilia et al. 2020). With a view to more ecofriendly production activities, ecogreases are becoming of extreme importance, for example, in wind turbines or farm machinery, among others. One feasible option is the use of vegetable sources as base oil (Almasi et al. 2021). Availability, biodegradability, non-toxicity and low price make vegetable oils a good choice. Sajeeb and Rajendrakumar (2019) compared the cost incurred for the use of conventional mineral oil with that for vegetable (coconut/mustard) oils. Total cost savings by replacing mineral oil with a blend (50/50) of both vegetable oils was estimated to be $0.77 per liter. Castor oil, with high viscosity and good thermal stability, results of special interest. Castor oil was found to remain thermally stable up to around 200 °C (Conceição et al. 2007). The production of vegetable oil-based

lubricants has been reported elsewhere (Almasi et al. 2021; Attia et al. 2020; Dehghani Soufi et al. 2019; Delgado et al. 2017; Durango-Giralfo et al. 2022; Fajardo et al. 2021; Heikal et al. 2017; McNutt and He 2016). However, as pointed out in Domínguez et al. (2021), the major challenge continues to be the substitution of the traditional thickeners (such as metallic soaps or polyureas). On these grounds, lignocellulosic materials and cellulosic derivatives have been shown to perform efficiently as thickening agents in vegetable oil (Borrero-López et al. 2018; Cortés-Triviño et al. 2019; Delgado et al. 2020a; Domínguez et al. 2021; Fajardo et al. 2021; Gorbacheva et al. 2021; Martín-Alfonso et al. 2011; Sánchez et al. 2011a, b). However, in most cases chemical modification of the lignocellulosic materials and high content of such a particulate phase was required. By way of examples, both Cortés-Triviño et al. (2019); Delgado et al. (2020a) examined the rheological and tribological behaviors of formulations based on castor oil and epoxidized cellulose pulp, which were found to depend on pulp modification degree and the epoxide compound. Borrero-López et al. (2018) described the linear viscoelastic behavior of wheat straw soda lignins (WSLs) NCO-functionalized with 1,6-hexamethylene diisocyanate and then dispersed in castor oil at a concentration as high as 25 wt%. Moreover, some of these formulations showed noticeable variations on both their rheological and tribological behaviors within a narrow temperature range below 100 °C. For example, Sánchez et al. (2011a) found a remarkable decrease in the plateau modulus G_N^0 as temperature was raised from 25 to 75 °C for oleogels based on methyl cellulose/ethyl cellulose blends in castor oil at 27 wt% cellulosic derivatives and ethyl to methyl weight ratios equal to or higher than 0.08. Cellulosic nanomaterials have also been used in lubricants. Awang et al. (2019) carried out an experimental study on characterization, stability and viscosity analysis of a nano-lubricant based on cellulose nanocrystals (CNC) suspended in SAE 40 engine oil. The oil viscosity slightly decreased with addition of 0.5 wt% CNC. Li et al. (2019) evaluated the friction-reducing properties of 2 wt% stearoyl chains grafted-cellulose nanocrystals in polyalphaolefin base oil, which was found to reduce the coefficient of friction (COF) by 30%. In Roman et al. (2021), an oleogel based on 1.4 wt% CNF (cellulose nanofibrils) in castor oil was demonstrated to have a viscoelastic behavior very similar to a commercial lubricating grease (8 wt% lithium soap thickener) with comparable NLGI consistency. Moreover, an electro-active lubricating oleogel based on cellulose nanofibers and castor oil was investigated by Delgado et al. (2020b).

Cellulose nanofibrils (CNFs) have been proved to be a powerful natural thickener (Foster et al. 2018). Due to their production method, cellulose nanofibers remain in aqueous solution upon nanofibrillation. Unfortunately, wet nanofibers are not compatible with vegetable oil. However, full water removal yields their irreversible aggregation (Ding et al. 2018). Hence, their potential application in lubricants requires a method of dispersion in vegetable oil. It has been found that cellulose nanofibrils oleogels can be efficiently produced using a solvent exchange method based on methanol which preserve their thickening capacity intact (Roman et al. 2021).

Homogenizing, grinding, twin-screw extrusion, cryo-crushing, and high-intensity ultrasonication are among the mechanical methods to manufacture CNFs (Xie et al. 2018). In order to save energy, pulp refining using PFI (Paper and Fiber Research Institute) mills or disks refiners may be performed prior to microfluidization. A better option is the oxidation with TEMPO (2,2,6,6-tetramethylpiperidine-1-oxyl radical) catalyst (Xie et al. 2018). Even though both pre-treatments (mechanical or chemical) yield nanofibers with very different surface properties, no research has been so far carried out on their effect on the thermo-rheological behavior of their castor oil-based oleogels.

The performance of lubricating greases is limited by the intensive thermal and mechanical conditions imposed (Delgado et al. 2006; Jiabao et al. 2020). Specific conditions can be found in the standard DIN 51825 for different types of lubricating greases. Extreme temperature fluctuations due to friction may shorten the lubricant lifetime. In the same way, the lubricant may be severely affected if, after being deformed well beyond its linear viscoelastic regime, it lacks capacity to return to their previous state at rest (Paszkowsky and Olsztynska-Janus 2014).

This research was intended to examine the rheological behavior of two ecofriendly lubricating greases based on castor oil and two types of cellulose nanofibers. Viscous flow and small amplitude oscillatory shear (SAOS) tests up to 180 °C were

done in order to establish a comparative analysis with traditional greases using metallic soap thickeners. The effect of the nanofibrillation pre-treatment, either mechanical or chemical, on the greases microstructure was evaluated through large amplitude oscillatory shear (LAOS) tests and SEM imaging.

Materials and methods

Raw materials

Castor oil, supplied by Guinama (Spain), was used as base oil. Its kinematic viscosity at 40 °C was 242.5 cSt. Other details can be found elsewhere (Ogunniyi 2006).

Two kinds of cellulose nanofibers from the same elm wood bleached pulp were kindly provided by Forest Research Centre, INIA-CSIC, Madrid (Spain): (a) cellulose nanofibers produced by PFI refining prior to microfluidization (CNF-PFI); (b) cellulose nanofibers obtained by TEMPO-mediated oxidation prior to microfluidization (CNF-TO). Their production process and characterization (chemical, morphological and surface chemistry) is detailed in Jiménez-López et al. (2020).

Oleogels preparation

The starting material consisted in cellulose nanofibers in the form of gel-like water suspensions with about 2 wt% solid content. CNFs incorporation into castor oil entailed a solvent exchange method using methanol. The methanol/hydrogel weight ratio used was 3/1. The oleogels were prepared at 1.4 wt% nanofibers. A T25 digital Ultra-Turrax homogenizer (25 °C, 10 min; and 10000 rpm) enabled an intimate mixing between the wet CNFs and the methanol solvent. Further centrifugation (in Thermo Scientific™ Sorvall™ ST 8 Small Benchtop Centrifuge) for 10 min and at 4000 rpm allowed a methanol-wetted nanocellulose precipitate to be separated from a water/methanol supernatant. This stage was repeated until water was fully removed from the nanofibers, which was monitored by using TGA runs. Afterwards, the precipitate was transferred into a round flask containing the castor oil and manually dispersed for 10 min. Finally, the remaining traces of methanol were eliminated under vacuum (Heidolph Laborota 4001 Rotary Evaporator) for 60 min, at 60 rpm and 60 °C, resulting an oleogel ready to be characterized.

Oleogels characterization

All oleogels were rheologically characterized using a rough plate-and-plate geometry (25 mm diameter and 1 mm gap) coupled to a controlled-stress rheometer Physica MCR-301 (Anton Paar, Austria), as described in Roman et al. (2021). Rough plates were used in order to avoid the wall slip phenomenon during the viscous flow measurements (Balan and Franco 2001). Small amplitude oscillation tests (SAOS) were carried out to evaluate the oleogels' elastic and viscous moduli within the linear viscoelastic (LVE) range, between 0.08 and 100 rad/s, and at selected temperatures between 25 and 180 °C. This temperature range was selected according to the most common operating temperature conditions reported in DIN 51,825. The LVE range was previously identified through oscillatory shear stress sweep tests at a constant frequency of 6.28 rad/s (1 Hz), at the different temperatures. Moreover, their viscous flow behavior, within the temperature range from 25 to 180 °C, was assessed between 10^{-2} and 10^{2} s^{-1}.

Moreover, the oleogels were also subjected to large amplitude oscillatory shear (LAOS) conditions with the purpose of evaluating their mechanical stability. According to Roman et al. (2022), all samples were evaluated according to a protocol consisting in three consecutive oscillatory shear time sweeps, at 1 Hz and 25 °C: (a) 5 min within the LVE regime (1 Pa); (b) 30 min outside the LVE regime; (c) 30 min again within the LVE regime. The first step provided the complex modulus value associated to the unaltered state of the sample, $|G_0^*|$; the second step yielded partial damage in the sample, reflected by the complex modulus value $|G_1^*|$; during the third step the initial state was partially recovered, $|G_2^*|$. Three non-linear stress values were arbitrarily selected: 20 (onset of the non-linear regime), 100 and 200 Pa.

Three replicates were carried out on fresh samples in order to ensure statistical significance at the 95% confidence level.

The oleogels' morphology was studied, at a magnification of ×7000, with a scanning electron microscope (SEM), model ZEISS EVO LS15 (ZEISS, Germany), at 10 kV, according to Roman

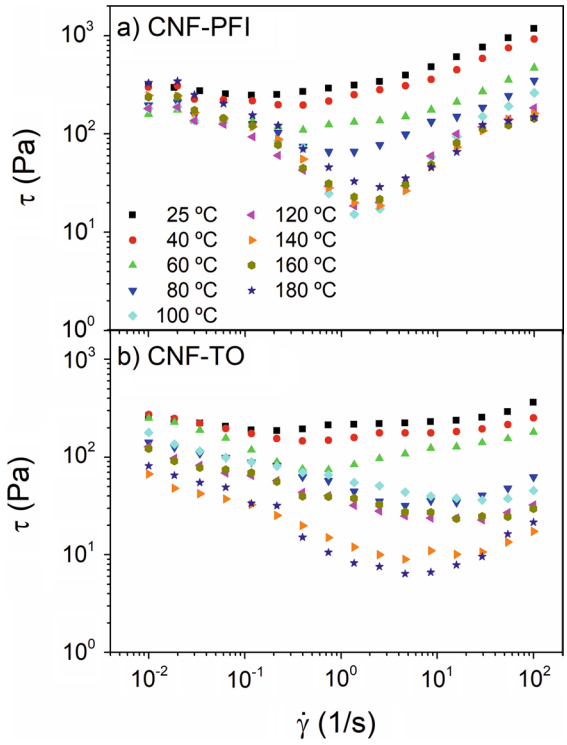

Fig. 1 Evolution of shear stress with shear rate, at different temperatures between 25 and 180 °C: **a** CNF-PFI oleogel; **b** CNF-TO oleogel

et al. (2021). Previously, castor oil was properly extracted from the oleogels, with no disturbance of the nanocellulose-based structural skeleton, by using the chemical fixation protocol described in Roman et al. (2021). The method consists of a first fixation using 5 wt% glutaraldehyde in 0.1 M cacodylate buffer, a second fixation with 1 wt% osmium tetraoxide solution, and final critical point drying in acetone before being metallized with Au/Pd. Representative morphology prototypes were assured by using, for each formulation studied, at least three different samples and taking five pictures at different locations.

A FT/IR-4200 spectrometer (JASCO) was used to obtain FTIR spectra with a wavenumber range from 500 to 4000 cm^{-1} in transmission mode. All samples were analyzed as thin layers on KBr disks (32 mm × 3 mm).

Results and discussion

Steady-state viscous flow behavior of cellulose nanofibrillated-based oleogels

Figure 1 displays the oleogels' flow curves, i.e., shear stress versus shear rate, at selected temperatures between 25 and 180 °C.

Regarding the CNF-PFI oleogel (Fig. 1a), its viscous flow behavior at the two lowest temperatures, 25 and 40 °C, was characterized by the presence of a yield stress of about 300 Pa at low shear rate values. In practice, this value stands for the onset of flow, and it is similar to those found in traditional lubricating greases (Delgado et al. 2019) which, at 25 °C, ranged from 500 to 1000 Pa, for a set of the aluminium-, lithium-, calcium- and polyurea-based greases. Upon flow commenced, pseudoplastic behavior was noticed. Interestingly, a minimum in the flow curve was detected with increasing temperature at intermediate shear rate values. According to Britton and Callaghan (1997), higher temperatures would cause noticeable structural changes in the oleogel's network which modify the velocity profile, thereby yielding manifested instabilities. However, at higher shear rates cellulose nanofibrils, were allowed to freely orientate during their flow, reducing the observed anomalous flow pattern.

With regard to the CNF-TO oleogel, Fig. 1b shows that its yielding behavior prevailed up to much higher shear rates such that, at 25 and 40 °C, the plateau zone extended over almost the entire curve. Moreover, the minimum shear stress value shifted to significantly higher shear rates as compared to the CNF-PFI oleogel.

Chemical interpretation based on potential interactions and SEM imaging

Different types of secondary interactions existing between the amphiphilic molecules involved are known to cause the extraordinary thickening capacity of nanocellulose in castor oil (Roman et al. 2022). Among them, hydrogen bonding is probably the most decisive. Interactions between the –OH on a glucose unit of cellulose with other cellulose chains and

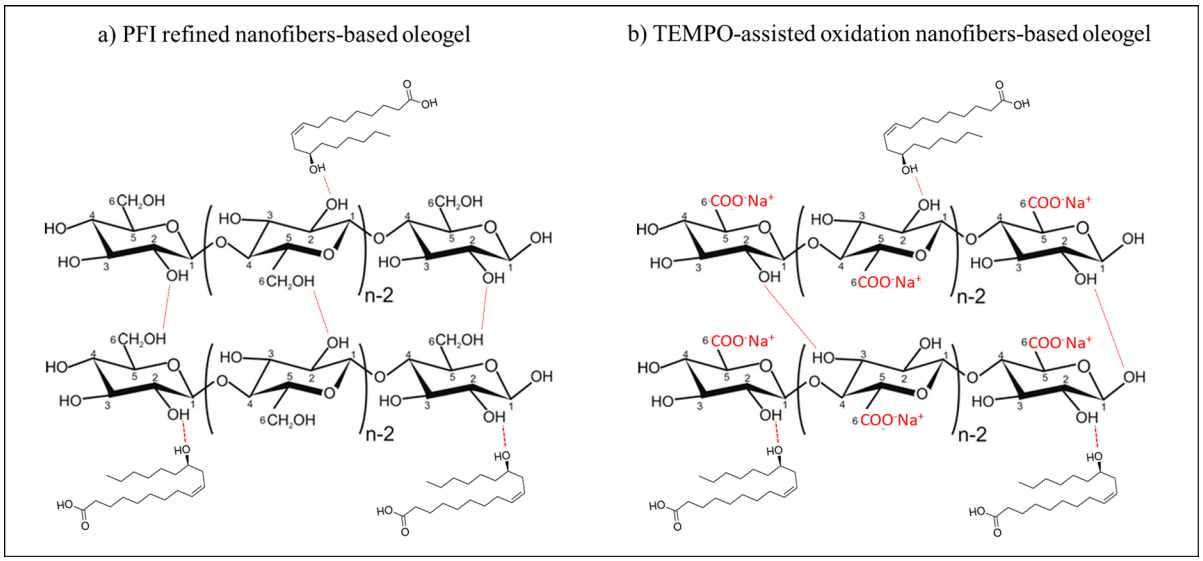

Fig. 2 Cellulose nanofibrils-based oleogels' structures, as derived from: **a** CNF-PFI; **b** CNF-TO

Table 1 Chemical composition of the cellulose nanofibrils studied

Type	Glucan (wt%)	Xylan (wt%)	Glucuronic ac. (wt%)	Total lignin (wt%)
CNF-PFI	82.6 ± 0.1	14.7 ± 0.1	1.0 ± 0.2	1.7 ± 0.3
CNF-TO	65.4 ± 0.2	10.5 ± 0.1	22.9 ± 0.7	1.2 ± 0.1

with the –OH on the ricinoleic acid of castor oil, as depicted in Fig. 2a, may yield gelification. H-bonds gradually become weaker with increasing temperature (Watanabe et al. 2006), thereby enhancing the so-called shear banding phenomenon.

On the other hand, elm wood pulp TEMPO-catalyzed oxidation was found to provoke crucial chemical changes in the nanofibrils. An outstanding increase in glucuronic acid, relative to that present in CNF-PFI, was found for CNF-TO as a result of the conversion of the C6 primary hydroxyl groups of cellulose into carboxylic groups (Table 1). A glucuronic acid content of 22.9 wt% was obtained for CNF-TO, as compared to 1 wt% for the CNFs derived from the PFI mechanical pretreatment. It is worth noting that in CNF-TO nanofibers glucuronic acid appears in the form of sodium glucuronate, as shown in Fig. 2b, because the TEMPO-catalyzed oxidation was carried out in the presence of various sodium species such as NaBr and NaClO (Fillat et al. 2018). In aqueous medium and under the resulting alkaline pH, the sodium carboxylate groups corresponding to the glucuronic units appear as carboxylate anions. Hence, strong electrostatic repulsion between fibrils arises, which prevent aggregation between adjacent fibrils, thereby enhancing the subsequent nanofibrillation stage. Table 2 shows the much greater ζ-potential of CNF-TO as compared to the PFI refined CNFs.

Upon transferring the nanofibrils into a non-polar aprotic medium such as castor oil, the sodium carboxylate groups remain as such (no anions are formed). In that sense, Doan et al. (1997) reported the dimerization of carboxylic sodium salts in anhydrous fluid medium. Dimerization occurs in a similar way to that between carboxylic acids, which can act as both hydrogen bond acceptors, due to their carbonyl group, and hydrogen bond donors, due to their hydroxyl group. However, in the case of their salts, dimers are formed by high-energy Coulombic interactions of their charged constituents rather than through hydrogen bonding.

FTIR analysis in Fig. 3 for the CNF-TO oleogel may shed some more light on the issue. Castor oil has been included in the analysis for the sake of comparison. The band at ca. 1654 cm^{-1}, which according to

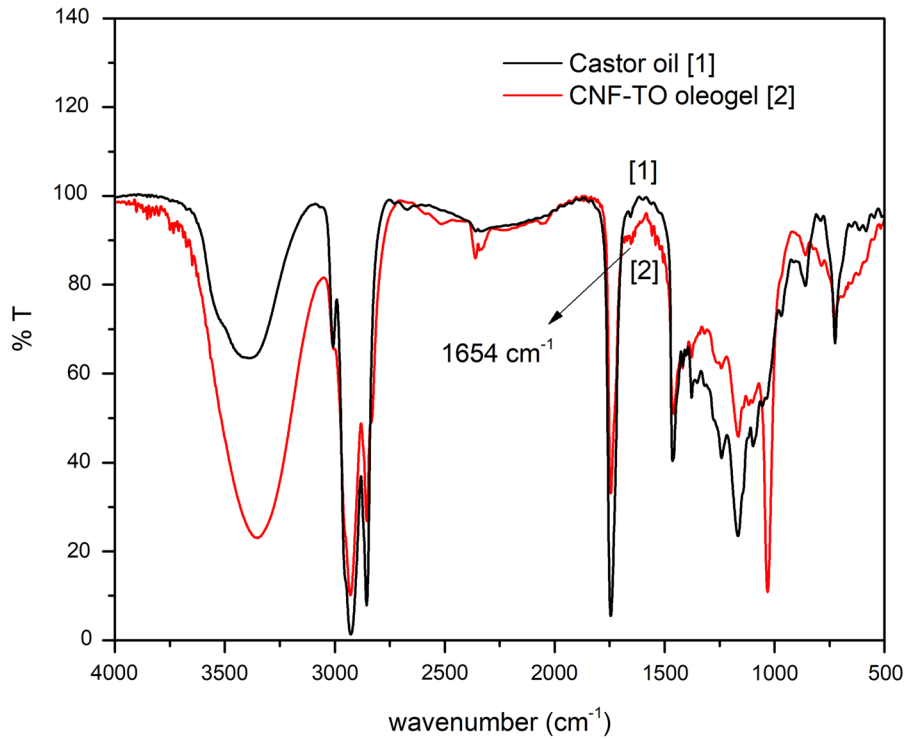

Fig. 3 Fourier-transform IR spectroscopy for the CNF-TO oleogel (red line). Castor oil added for the sake of comparison (black line)

Doan et al. (1997) corresponds to carbonyl stretching frequencies of R-COO$^-$Na$^+$ in the < salt-salt > dimers, would support the proposed model for the CNF-TO olegel depicted in Fig. 2b. In consequence, a tighter microstructure, involving the dimerization of adjacent sodium carboxylate groups, i.e., much stronger interactions than simple hydrogen bonds in PFI refined nanofibers, seems to have formed with TEMPO-assisted oxidation nanofibers. This type of inter-chain interactions would have extended the yielding behavior of the CNF-TO oleogel up to much larger shear rates. In turn, they would have made it more sensitive to temperature as compared to the PFI refined nanofibers-based oleogels.

A microstructural characterization, conducted by Scanning Electron Microscopy (SEM), is shown in Fig. 4. Figure 4a for the CNF-PFI oleogel displays an entangled network constituted by both individual nanofibers and non-nanofibrillated microfibrils. Conversely, Fig. 4b reveals that a part of the CNF-TO nanofibers seems to have agglomerated upon being transferred to the oil. Such a network microstructure might be a consequence of abundant sodium carboxylate groups onto the nanocellulose surface. Based on the species formed upon the oxidation process involving TEMPO catalyst, the FTIR analysis and visual inspection of Fig. 4, we hypothesize a dimerization process by Coulombic interactions. The nanofibrillation pre-treatment, in terms of conversion of cellulose primary -OH groups into –COO$^-$Na$^+$ groups, seems to affect remarkably the oleogels' microstructure. This outcome highlights the importance of the nanofibers surface chemistry in the rheological behavior of their suspensions (Moberg et al. 2017), placing special emphasis on the influence of intermolecular forces in the way fibrils arrange.

Moreover, their high value of ζ-potential in aqueous medium yielded an improved nanofibrillation performance. Hence, the final CNF-TO oleogel presented 100% nano-sized fibrils, as compared to PFI-refined CNFs with only 60% nano-sized fibrils

Table 2 Selected characteristics of the cellulose nanofibrils studied

Type	Fibrillation yield (%)	ζ-potential (mV)	D (nm)	L (nm)
CNF-PFI	60.8 ± 2.5	− 28.4	5.9 ± 1.7	1237 ± 680
CNF-TO	100	− 68.1	2.6 ± 0.7	700 ± 160

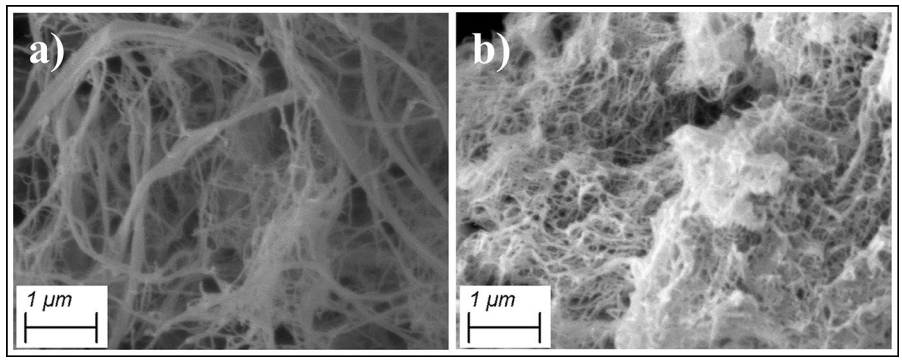

Fig. 4 SEM imaging on cellulose nanofibers-based oleogels: **a** CNF-PFI; **b** CNF-TO

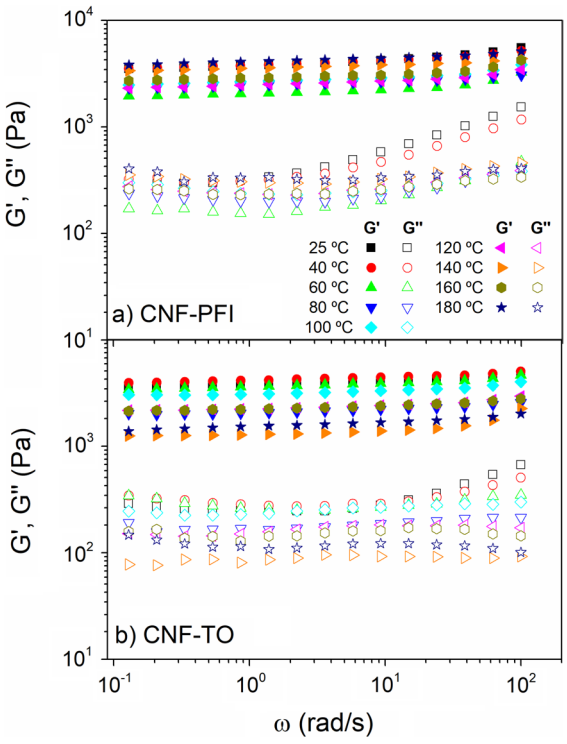

Fig. 5 Evolution of the linear storage (G′) and loss (G″) moduli with frequency, within the temperature range from 25 to 180 °C: **a** CNF-PFI; **b** CNF-TO

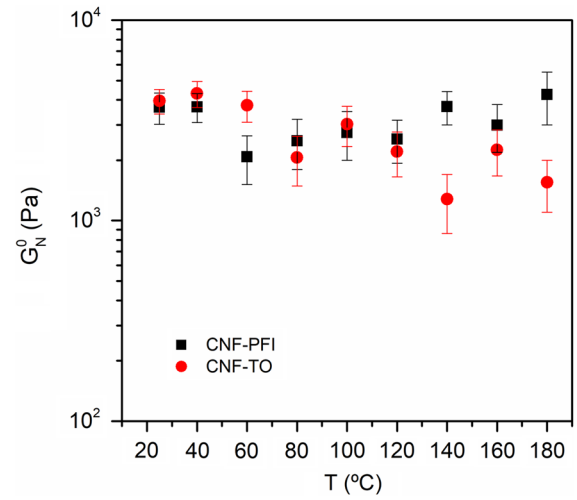

Fig. 6 Temperature dependency of the plateau modulus, G_N^0

(Jiménez-López et al. 2020), whilst their average length and diameter also changed very significantly (Table 2). In consequence, their different rheological behavior might also be associated to the existing change in fibril morphology (Moberg et al. 2017).

Linear viscoelastic behavior of cellulose nanofibrillated-based oleogels

Figure 5 shows the results of small amplitude oscillatory shear measurements as a function of temperature (25–180 °C). They correspond to the so-called physical gel, that is, a shear storage modulus (G′) which exhibits a pronounced plateau extending to times of the order of seconds, and a loss modulus (G″) which is considerably smaller than the storage modulus in this region (Ross-Murphy 1994). Physical gels consist of chains "physically" cross-linked into networks, and possess properties of both chemically cross-linked materials and entanglement networks (pseudo-gel). As stated in Ross-Murphy (1995), physical gels involve the presence of one or more of the following

non-covalent cross-links: Coulombic, dipole-dipole, van der Waals, charge transfer, and hydrophobic and hydrogen bonding interactions. Regarding the CNF-PFI oleogel (Fig. 5a), a notorious minimum in the loss modulus was observed at 25 and 40 °C. Such a minimum became less noticeable as temperature was increased. In contrast, the loss modulus curves corresponding to the CNF-TO oleogel became largely independent of frequency (nearly flat) with increasing temperature. Hence, under SAOS conditions, this oleogel exhibited a stronger gel-like behavior, as compared to the CNF-PFI oleogel which was more akin to entanglement networks, that is, pseudogels (Ross-Murphy 1995.

It is interesting to note that conventional lubricating greases and greases based on other types of biopolymers rather than nanocellulose also behave like gels. However, the observed temperature-dependency in Fig. 5 was quite different to them. Thus, the evolution with temperature of the so-called plateau modulus, G_N^0 (G′ value at the frequency value corresponding to the G″ minimum) is shown in Fig. 6. Such a parameter is a measure of the strength of the gel-like structure. For a standard lithium-based lubricating grease, 110 °C was found to be the onset of important microstructural changes, as deduced from an abrupt decay when G_N^0 was plotted against temperature (Delgado et al. 2006). Moreover, Sánchez et al. (2011a) analyzed the plateau modulus-temperature dependence of cellulosic derivatives thickeners in castor oil. They observed a remarkable decrease in G_N^0 with temperature, which was attributed to the sol-gel transition of ethyl cellulose in castor oil at around 70 °C. On the contrary, Fig. 6 demonstrates quite acceptable stability of G_N^0 all over the entire temperature interval studied (up to 180 °C).

By comparing Figs. 1 and 5, it can be concluded that the above described (H-bonding and Coulombic) interactions are less sensible to small deformations associated to linear viscoelasticity measurement as compared to viscous flow tests which entails much larger deformations. However, at low shear rates on the flow curve, the applied deformations can be also small. For that reason, the evolution with temperature of the elastic modulus (Fig. 5) and the yield stress (Fig. 1) are similar. In both cases, the CNF-TO oleogel presents a higher temperature sensitivity than the CNF-PFI oleogel. The evolution of G_N^0 with temperature, in Fig. 6, also reveals this result.

Table 3 Destruction and recovery percentages of the nanocellulose-based oleogels studied, after samples were submitted to different shear stress levels outside the LVE region

Oleogel	Non-linear stress value (Pa)	%-destruction	%-recovery
CNF-PFI	100	41.4	54.1
	200	55.7	52.0
CNF-TO	100	95.8	25.8
	200	98.6	13.4

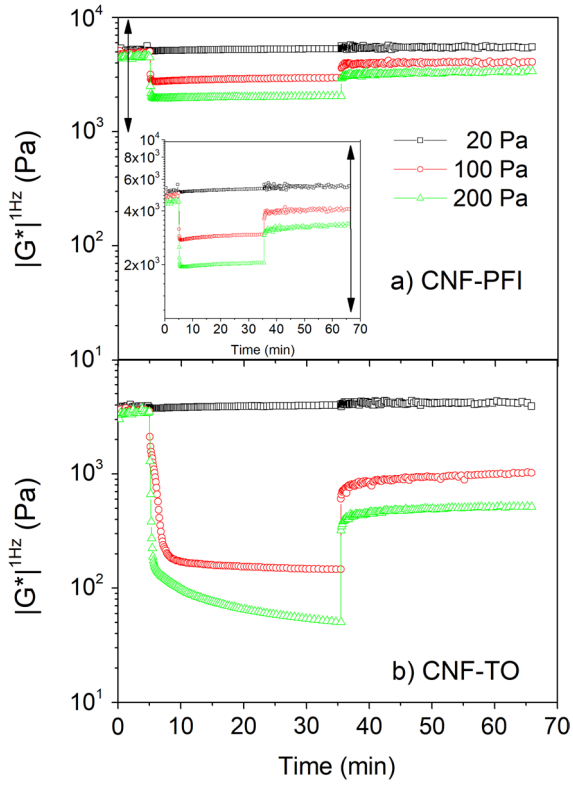

Fig. 7 Time evolution of the dynamic shear modulus, $|G^*|$, at 1 Hz and 25 °C, at selected shear stress values outside the LVE region: **a** CNF-PFI (inset with enlarged scale); **b** CNF-TO

Susceptibility to large amplitude oscillatory shear (LAOS) of cellulose nanofibrillated-based oleogels

Ability to flow under mechanical stresses with no detriment of their shear stability are among the features which are mainly demanded from a lubricating grease (Adhvaryu et al. 2005). Through previous viscous flow and small amplitude oscillatory shear (SAOS) tests, it was concluded that shear

and temperature affected the oleogels' rheological behavior in different ways depending on cellulose nanofibrillation pre-treatment. The application of a shear stress beyond the LVE region induces a certain degree of non-reversible structural breakdown, resulting in the disturbance of the grease's lubrication capacity (Paszkowsky and Olsztynska-Janus 2014). In order to look further into this issue, the oleogels were subjected to tests which measured their resilience to non-linear stresses and their ability to recover their initial state.

Figure 7 displays the log-linear evolution of the norm of the complex shear modulus $|G^*|$, at a selected frequency of 1 Hz, against time, at different stresses. A linear stress of 1 Pa was applied during the first 5 min. Over that period, the material's intrinsic microstructure was unaffected in such a way that $|G^*|$ was exactly the same for the three experiments. Then, the corresponding non-linear stress was input and maintained for a period of 30 min. An instant decay in $|G^*|$ was observed. "Rheo-destruction" percentages, defined as the ratio of $|G_0^*|$–$|G_1^*|$ relative to $|G_0^*|$, are displayed in Table 3. Small effect was found at 20 Pa, the onset of the LVE regime (not included in Table 3). Further this threshold, severe destruction with increasing the stress value was monitored.

Furthermore, partial recovery was observed when the material was returned to the LVE. ''Rheo-recovery'' percentages were calculated as the ratio of $|G_2^*|$–$|G_1^*|$ relative to $|G_0^*|$–$|G_1^*|$ and shown in Table 3.

As shown in Fig. 7, very pronounced differences were observed between the PFI refined (fully mechanical production) nanofiber and the TEMPO-mediated oxidated (chemically-assisted production) nanofiber. The CNF-PFI oleogel exhibited lower values of %-destruction (41.4% at 100 Pa) and larger values of %-recovery (54.1% at 100 Pa). On the contrary, very large %-destruction and very small %-recovery were found both at 100 and 200 Pa for the CNF-TO oleogel. It results very interesting to note that, at 200 Pa, its $|G^*|$ continue to steadily decrease all over the non-linear stage (30 min) upon the initial instant decay. Based on a dissipated energy approach, the curve of the so-called dissipated energy ratio versus number of cycles (not shown) moves away from the linear viscoelastic damping asymptote. This result would suggest that non recoverable fatigue damage was experienced by the CNF-TO oleogel's network by application of repetitive loading (Frigio et al. 2016). In that way, a long loading time may be expected to yield irreversible fatigue failure.

The applied chemical pre-treatment seems to have contributed to a nanofiber surface chemistry which endows the oleogel with much higher sensitivity to large shear deformations. As previously remarked, in comparison with the two other nanofibers, the above mentioned Coulombic interactions between sodium carboxylate groups might be performing as semi-permanent junction points. In that sense, the CNF-PFI oleogel, constituted by physical crosslinking and inter-chain hydrogen bonding, may still relax and accommodate to the application of large deformations (Roman et al. 2022). In turn, in the CNF-TO oleogel, its flow process would be constrained by the existence of tougher inter-chains interactions through dimerization of sodium carboxylate groups involving Coulombic forces. Such interactions would eventually break up, thereby weakening their microstructure. Ross-Murphy (1995) stated that, when subjected to large deformations, strong gels will rupture and will never "heal" without melting and resetting, whereas the weak gels will recover given sufficient time. Hence, under LAOS conditions, the CNF-PFI oleogel behaved as a weak gel, whereas the CNF-TO oleogel was proved to be more akin to a strong gel. The non-linear response observed in Fig. 7 was found to be in direct relation to the ζ-potential values which the nanofibers had in alkaline aqueous medium (Table 2) before they were transferred into oil medium. Thus, CNF-PFI, with a lower (in absolute value) ζ-potential of −28.4 mV, showed lower shear-sensitivity, whereas CNF-TO, with larger ζ-potential of −68.1 mV, was more sensitive. Moreover, there also seems to be some correlation with the temperature evolution of the yield stress in the viscous flow tests, where CNF-TO was more sensitive than CNF-PFI (Fig. 1).

Conclusions

Viscous flow and dynamic shear tests enabled a distinction to be made between both types of oleogels. As compared to the CNF-PFI oleogel, which was shown to be more akin to an entanglement network, the CNF-TO oleogel exhibited a noticeable gel-like behavior. The rheological behavior of the CNF-PFI oleogel was attributed to a nanofiber network mainly

involving typical inter-molecular hydrogen bonding of entangled fibrils, which may freely orientate under large deformations (weak gel). In turn, the CNF-TO oleogel would be restrained by tougher inter-chains interactions involving much stronger Coulombic forces. The microstructural characterization carried out on the CNF-PFI oleogel by Scanning Electron Microscopy (SEM) demonstrated entangled networks constituted by both individual nanofibers and of non-nanofibrillated microfibrils. Conversely, a part of the CNF-TO nanofibers seems to have agglomerated upon being transferred to the oil. Hence, under LAOS conditions, the CNF-TO oleogel presented larger values of %-destruction and lower values of %-recovery (strong gel).

These results have important implications with a view to the use of such nanofibers in the formulation of lubricating greases. It can be concluded that cellulose nanofibers from PFI refining physical pretreatment are a better option than those from TEMPO-mediated oxidation pretreatment in terms of lower thermal susceptibility and higher mechanical stability.

Acknowledgments Not applicable.

Author contributions MG-M and MAD made the most relevant contributions to the study conception and design, as well as to funding acquisition. Data collection is mainly attributed to CR and SDF-S. Material preparation and analysis were performed by all authors. The first draft of the manuscript was written by CR. All authors contributed significantly to the final version of the manuscript. Supervision was mainly carried out by MG-M. All authors read and approved the final manuscript.

Funding Funding for open access publishing: Universidad de Huelva/CBUA. This work is part of two Research Projects sponsored by "Programa Operativo FEDER-Andalucía 2014–2020" (UHU-1255843 and UHU-202008). The authors gratefully acknowledge their financial support. S.D. Fernández-Silva acknowledges "Ayudas para la Contratación Predoctoral de Personal Investigador en Formación 2021, Junta de Andalucía" (PREDOC_01696), for funding his PhD Thesis.

Availability of data and materials Data and materials will be made available on request from the corresponding author (moises.garcia@diq.uhu.es).

Declarations

Conflict of interest All authors declare that they have no conflict of interest.

Ethics approval and consent to participate Not applicable.

Consent for publication Not applicable.

References

Adhvaryu A, Sung C, Erhan SZ (2005) Fatty acids and antioxidant effects on grease microstructures. Ind Crops Prod 21:285–291. https://doi.org/10.1016/j.indcrop.2004.03.003

Almasi S, Ghobadian B, Najafi G, Soufi MD (2021) A novel approach for bio-lubricant production from rapeseed oil-based biodiesel using ultrasound irradiation: multi-objective optimization. Sustain Energy Technol Assess 43:100960. https://doi.org/10.1016/j.seta.2020.100960

Attia NK, El-Mekkawi SA, Elardy OA, Abdelkader EA (2020) Chemical and rheological assessment of produced biolubricants from different vegetable oils. Fuel 271:117578. https://doi.org/10.1016/j.fuel.2020.117578

Awang NW, Ramasamy D, Kadirgam K, Samykano M, Najafi G, Sidik NAC (2019) An experimental study on characterization and properties of nano lubricant containing cellulose nanocrystal (CNC). Int J Heat Mass Transf 130:1163–1169. https://doi.org/10.1016/j.ijheatmasstransfer.2018.11.041

Balan C, Franco JM (2001) Influence of the geometry on the transient and steady flow of lubricating greases. Tribol Trans 44:53–58. https://doi.org/10.1080/10402000108982426

Bart JCJ, Gucciardi E, Cavallaro S (2013) Lubricants: properties and characteristics. In: Bart JCJ, Gucciardi E, Cavallaro S (eds) Biolubricants Science and Technology. Woodhead Publishing, Cambridge, pp 24–73

Borrero López AM, Blánquez A, Valencia C, Hernández M, Arias ME, Eugenio ME, Fillat U, Franco JM (2018) Valorization of soda lignin from wheat straw solid-state fermentation: production of oleogels. ACS Sustain Chem Eng 6:5198–5205. https://doi.org/10.1021/acssuschemeng.7b04846

Britton MM, Callaghan PT (1997) NMR visualisation of anomalous flow in cone-and-plate rheometry. J Rheol 41:1365–1386. https://doi.org/10.1122/1.550846

Cecilia JA, Ballesteros D, Alves RM, Murilo F, Cavalcante E Jr (2020) An overview of the biolubricant production

process: challenges and future perspectives. Processes 8:257. https://doi.org/10.3390/pr8030257
Conceição MM, Fernandes VJ, Araújo AS, Farias MF, Santos IMG, Souza AG (2007) Thermal and oxidative degradation of castor oil biodiesel. Energy Fuels 21(3):1522–1527. https://doi.org/10.1021/ef0602224
Cortés-Triviño E, Valencia C, Delgado MA, Franco JM (2019) Thermo-rheological and tribological properties of novel bio-lubricating greases thickened with epoxidized lignocellulosic materials. J Ind Eng Chem 80:626–632. https://doi.org/10.1016/j.jiec.2019.08.052
Dehghani Soufi M, Ghobadian B, Mousavi SM, Najafi G, Aubin J (2019) Valorization of waste cooking oil based biodiesel for biolubricant production in a vertical pulsed column: energy efficient process approach. Energy 189:116266. https://doi.org/10.1016/j.energy.2019.116266
Delgado MA, Cortés-Triviño E, Valencia C, Franco JM (2020) Tribological study of epoxide-functionalized alkali lignin-based gel-like biogreases. Tribol Int 146:106231. https://doi.org/10.1016/j.triboint.2020.106231
Delgado MA, Fernández-Silva SD, Roman C, García-Morales M (2020) On the electro-active control of nanocellulose-based functional biolubricants. ACS Appl Mater Interfaces 12:46490–46500. https://doi.org/10.1021/acsami.0c12244
Delgado MA, Quinchia LA, Spikes HA, Gallegos C (2017) Suitability of ethyl cellulose as multifunctional additive for blends of vegetable oil-based lubricants. J Clean Prod 151:1–9. https://doi.org/10.1016/j.jclepro.2017.03.023
Delgado MA, Secouard S, Valencia C, Franco JM (2019) On the steady-state flow and yielding behaviour of lubricating greases. Fluids 4:6. https://doi.org/10.3390/fluids4010006
Delgado MA, Valencia C, Sánchez MC, Franco JM, Gallegos C (2006) Thermorheological behaviour of a lithium lubricating grease. Tribol Lett 23:47–54. https://doi.org/10.1007/s11249-006-9109-5
Ding Q, Zeng J, Wang B, Tang D, Chen K, Gao W (2018) Effect of nanocellulose fiber hornification on water fraction characteristics and hydroxyl accessibility during dehydration. Carbohydr Polym 207:44–51. https://doi.org/10.1016/j.carbpol.2018.11.075
Doan V, Kolppe R, Kasai PH (1997) Dimerization of carboxylic acids and salts: an IR study in perfluoropolyether media. J Am Chem Soc 119:9810–9815. https://doi.org/10.1021/ja970304u
Domínguez G, Blánquez A, Borrero-López AM, Valencia C, Eugenio ME, Arias ME, Rodríguez J, Hernández M (2021) Eco-friendly oleogels from functionalized Kraft Lignin with laccase SilA from Streptomyces ipomoeae: an opportunity to replace commercial lubricants. ACS Sustain Chem Eng 9:4611–4616. https://doi.org/10.1021/acssuschemeng.1c00113
Durango-Giraldo G, Zapata-Hernández C, Santa JF, Buitrago-Sierra R (2022) Palm oil as a biolubricant: literature review of processing parameters and tribological performance. J Ind Eng Chem 107:31–44. https://doi.org/10.1016/j.jiec.2021.12.018
Fajardo C, Blánquez A, Domínguez G, Borrero-López AM, Valencia C, Hernández M, Arias ME, Rodríguez J (2021) Assessment of sustainability ofBio treated lignocellulose-based oleogels. Polymers 13:267. https://doi.org/10.3390/polym13020267
Fillat U, Wicklein B, Martín-Sampedro R, Ibarra D, Ruiz-Hitzky E, Valencia C, Sarrión A, Castro E, Eugenio ME (2018) Assessing cellulose nanofiber production from olive tree pruning residue. Carbohydr Polym 179:252–261. https://doi.org/10.1016/j.carbpol.2017.09.072
Foster EJ, Moon RJ, Agarwal UP et al (2018) Current characterization methods for cellulose nanomaterials. Chem Soc Rev 8:1–71. https://doi.org/10.1039/C6CS00895J
Frigio F, Ferrotti G, Cardone F (2016) Fatigue rheological characterization of polymer-modified bitumens and mastics. In: Canestrari F, Partl MN (eds) Proceedings 8th RILEM international symposium on testing and characterization of sustainable and innovative bituminous materials, RILEM Bookseries 11. Springer, New York, pp 655–666
Gorbacheva SN, Yadykova AY, Ilyin SO (2021) Rheological and tribological properties of low-temperature greases based on cellulose acetate butyrate gel. Carbohydr Polym 272:118509. https://doi.org/10.1016/j.carbpol.2021.118509
Heikal EK, Elmelawy MS, Khalil SA, Elbasuny NM (2017) Manufacturing of environment friendly biolubricants from vegetable oils. Egypt J Pet 26:53–59. https://doi.org/10.1016/j.ejpe.2016.03.003
Jiabao P, Guangxin Y, Jianpin W (2020) Effect of thermorheological properties on tribological behaviors of lubricating grease. Mater Res Express 7:035509. https://doi.org/10.1088/2053-1591/ab81bc
Jiménez-López L, Eugenio ME, Ibarra D, Darder M, Martín JA, Martín-Sampedro R (2020) Cellulose nanofibers from a Dutch Elm disease-resistant *Ulmus minor* clone. Polymers 12:2450. https://doi.org/10.3390/polym12112450
Li K, Zhang X, Du C, Yang J, Wu B, Guo Z, Dong C, Lin N, Yuan C (2019) Friction reduction and viscosity modification of cellulose nanocrystals as biolubricant additives in polyalphaolefin oil. Carbohydr Polym 220:228–235. https://doi.org/10.1016/j.carbpol.2019.05.072
Martín-Alfonso JE, Nuñez N, Valencia C, Franco JM, Díaz MJ (2011) Formulation of new biodegradable lubricating greases using ethylated cellulose pulp as thickener agent. J Ind Eng Chem 17:818–823. https://doi.org/10.1016/j.jiec.2011.09.003
McNutt J, He Q (2016) Development of biolubricants from vegetable oils via chemical modification. J Ind Eng Chem 36:1–12. https://doi.org/10.1016/j.jiec.2016.02.008
Moberg T, Sahlin K, Yao K, Geng S, Westman G, Zhou Q, Oksman K, Rigdahl M (2017) Rheological properties of nanocellulose suspensions: effects of fibril/particle dimensions and surface characteristics. Cellulose 24:2499–2510. https://doi.org/10.1007/s10570-017-1283-0
Ogunniyi DS (2006) Castor oil: a vital industrial raw material. Biores Technol 97:1086–1091. https://doi.org/10.1016/j.biortech.2005.03.028
Paszkowski M, Olsztynska-Janus S (2014) Grease thixotropy: evaluation of grease microstructure change due to shear and relaxation. Ind Lubr Tribol 66:223–237. https://doi.org/10.1108/ILT-02-2012-0014
Reeves CJ, Siddaiah A, Menezes PL (2017) A review on the science and technology of natural and synthetic

biolubricants. J Bio Tribo Corros 3:11. https://doi.org/10.1007/s40735-016-0069-5

Roman C, Delgado MA, Fernández-Silva SD, García-Morales M (2022) Exploring the effect of the pulp bleaching on the thermo-rheological behavior of sustainable cellulose nanofiber-based oleogels. J Environ Chem Eng 10:108617. https://doi.org/10.1016/j.jece.2022.108617

Roman C, García-Morales M, Eugenio ME, Ibarra D, Martín-Sampedro R, Delgado MA (2021) A sustainable methanol-based solvent exchange method to produce nanocellulose-based ecofriendly lubricants. J Clean Prod 319:128673. https://doi.org/10.1016/j.jclepro.2021.128673

Roman C, Valencia C, Franco JM (2016) AFM and SEM assessment of lubricating Grease microstructures: influence of sample preparation protocol, frictional working conditions and composition. Tribol Lett 63:20. https://doi.org/10.1007/s11249-016-0710-y

Ross-Murphy SB (1994) Rheological characterization of polymer gels and networks. Polym Gels Netw 2:229–237. https://doi.org/10.1016/0966-7822(94)90007-8

Ross-Murphy SB (1995) Structure-property relationships in food biopolymer gels and solutions. J Rheol 39:1451. https://doi.org/10.1122/1.550610

Sajeeb A, Rajendrakumar PK (2019) Comparative evaluation of lubricant properties of biodegradable blend of coconut and mustard oil. J Clean Prod 240:118255. https://doi.org/10.1016/j.jclepro.2019.118255

Sánchez R, Franco JM, Delgado MA, Valencia C, Gallegos C (2011) Thermal and mechanical characterization of cellulosic derivatives-based oleogels potentially applicable as bio-lubricating greases: influence of ethyl cellulose molecular weight. J Ind Eng Chem 17:705–711. https://doi.org/10.1016/j.jiec.2011.05.019

Sánchez R, Stringari GB, Franco JM, Valencia C, Gallegos C (2011) Use of chitin, chitosan and acylated derivatives as thickener agents of vegetable oils for bio-lubricant applications. Carbohydr Polym 85:705–714. https://doi.org/10.1016/j.carbpol.2011.03.049

Watanabe A, Morita S, Ozaki Y (2006) Temperature-dependent structural changes in hydrogen bonds in microcrystalline cellulose studied by infrared and near-infrared spectroscopy with perturbation-correlation moving-window two-dimensional correlation analysis. Appl Spectrosc 60:611–618. https://doi.org/10.1366/000370206777670549

Xie H, Du H, Yang X, Si C (2018) Recent strategies in preparation of cellulose nanocrystals and cellulose nanofibrils derived from raw cellulose materials. Int J Polym Sci 2018:7923068. https://doi.org/10.1155/2018/7923068